CrossMark

MR imaging features associated with distant metastasis-free survival of patients with invasive breast cancer: a case–control study

Sung Eun Song[1,2] · Sung Ui Shin[1] · Hyeong-Gon Moon[3] · Han Suk Ryu[4] ·
Kwangsoo Kim[5] · Woo Kyung Moon[1]

Abstract

Purpose Preoperative breast magnetic resonance (MR) imaging features of primary breast cancers may have the potential to act as prognostic biomarkers by providing morphologic and kinetic features representing inter- or intra-tumor heterogeneity. Recent radiogenomic studies reveal that several radiologist-annotated image features are associated with genes or signal pathways involved in tumor progression, treatment resistance, and distant metastasis (DM). We investigate whether preoperative breast MR imaging features are associated with worse DM-free survival in patients with invasive breast cancer.

Methods Of the 3536 patients with primary breast cancers who underwent preoperative MR imaging between 2003 and 2009, 147 patients with DM were identified and one-to-one matched with control patients ($n = 147$) without DM according to clinical–pathologic variables. Three radiologists independently reviewed the MR images of 294 patients, and the association of DM-free survival with MR imaging and clinical–pathologic features was assessed using Cox proportional hazard models.

Results Of MR imaging features, rim enhancement (hazard ratio [HR], 1.83 [95% confidence interval, CI 1.29, 2.51]; $p = 0.001$) and peritumoral edema (HR, 1.48 [95% CI 1.03, 2.11]; $p = 0.032$) were the significant features associated with worse DM-free survival. The significant MR imaging features, however, were different between breast cancer subtypes and stages.

Conclusion Preoperative breast MR imaging features of rim enhancement and peritumoral edema may be used as prognostic biomarkers that help predict DM risk in patients with breast cancer, thereby potentially enabling improved personalized treatment and monitoring strategies for individual patients.

Keywords Breast cancer · Magnetic resonance imaging · Neoplasm metastasis · Prognosis

✉ Woo Kyung Moon
  moonwk1963@gmail.com

1   Department of Radiology, Seoul National University Hospital, Seoul National University College of Medicine, 101 Daehak-ro, Jongno-gu, Seoul 110-744, Korea

2   Department of Radiology, Korea University College of Medicine, Seoul, Korea

3   Department of Surgery, Seoul National University Hospital and Cancer Research Institute, Seoul National University College of Medicine, Seoul, Korea

4   Department of Pathology, Seoul National University Hospital, Seoul National University College of Medicine, Seoul, Korea

5   Division of Clinical Bioinformatics, Biomedical Research Institute, Seoul National University Hospital, Seoul, Korea

Introduction

Despite progress in treatment, approximately 20–30% of early breast cancer patients develop distant metastasis (DM), which is related to the majority of deaths from breast cancer [1]. As it is difficult to accurately predict the risk of DM for individual patients using current prognostic markers, new biomarkers to stratify breast cancer outcome are needed to develop individualized therapy [2]. Established prognostic markers for DM include a younger age, a large tumor size, the presence of axillary nodal metastasis, a high histologic grade, lymphovascular invasion, a high

🖄 Springer

Ki-67 index, negative estrogen receptor (ER) expression, and human epidermal growth factor receptor 2 (HER2) overexpression [3–6]. Emerging data suggest the importance of breast cancer gene expression profiles and immunohistochemical (IHC) information to predict patient prognosis and guide treatment decisions [7, 8]. Women with a higher risk of early relapse appear to benefit from the use of novel or more intensive adjuvant treatment [9, 10].

Preoperative MR imaging features of primary breast tumors may have the potential to act as prognostic biomarkers by providing morphologic and kinetic features representing inter- or intra-tumor heterogeneity and the microenvironment [11]. Indeed, prior research has revealed relationships between MR imaging features, IHC subtypes, and clinical outcome of breast cancers [12–14]. Particularly, rim enhancement, defined as the strong enhancement at the periphery of a tumor compared with that at the center [13]; the presence of peritumoral edema displayed on T2-weighted images (T2WI) [14]; and the prepectoral location [15], appeared to be associated with aggressive tumor biology and a poor outcome. In addition, background parenchymal enhancement (BPE) was reported as a potential biomarker for poor outcome [16] and as a guide for therapy in HR-positive/HER2-negative breast cancer [17, 18]. However, previous studies of this subject did not include clinical or pathologically matched controls, used local or regional recurrence rather than DM as the survival outcome and included only patients undergoing conservation surgery or neoadjuvant chemotherapy. Furthermore, MR imaging features associated with DM-free survival according to IHC subtypes have not been described.

Therefore, the purpose of our study was to investigate whether preoperative breast MR imaging features are associated with worse DM-free survival in patients with invasive breast cancer.

Materials and methods

Study population

This retrospective study was approved by our institutional review board, and the requirement for obtaining informed consent was waived. From a review of our institution's database between September 2003 and June 2009, we retrospectively identified 4507 consecutive women who were newly diagnosed with invasive breast cancers and underwent preoperative breast MR imaging and treatment in our institution. Among them, we excluded the following women: those who had received neoadjuvant chemotherapy ($n = 537$) or surgical biopsy ($n = 24$) prior to MR imaging; those with incomplete IHC data including HER2

2+ score without fluorescence in situ hybridization (FISH) ($n = 337$); those with synchronous or metachronous contralateral cancer ($n = 63$); and those with metastatic disease on presentation ($n = 10$). Of the 3536 women (median age, 48.8 years old; age range, 18–85 years old), 147 (4.2%) were identified as having a DM as a first event without loco-regional recurrence. Distant metastasis did not include the cases with isolated ipsilateral or contralateral breast recurrence, isolated regional lymph node patients, or local chest wall recurrence. DM was confirmed by histopathologic analysis in 81 patients and by imaging and clinical follow-up in 66 patients.

To identify a control group for 147 women with DM of breast cancer, 9 covariates known as independent risk factors for DM [2–7] were one-to-one matched pairwise to each woman identified from the remaining 3389 women without DM, according to the following criteria: age (<50 years or ≥50 years), pathologic tumor type (ductal or lobular and others), histologic grade (I or II or III), pathologic tumor size (T1 or T2 or T3), pathologic nodal stage (N0 or N1 or N2-3), pathologic stage (I or II or III), lymphovascular invasion (absent or present), Ki-67 index (<14% or ≥14%), and IHC subtype (hormone receptor (HR)-positive/HER2-negative [ER and/or PR-positive and HER2-negative] or HER2-positive [ER/PR-positive or negative, HER2-positive] or triple-negative [ER-negative, PR-negative and HER2-negative]) [8], maximizing follow-up time over 5 years. Therefore, a total of 294 women (147 women with DM [DM group] and 147 matched women without DM [control group]) comprised our study population. The median follow-up period of patients in the control group ($n = 147$) was 6.3 years (range, 5–11.3 years).

MR imaging technique

All MR imaging examinations were performed using a 1.5-T scanner (Signa, GE Medical Systems, Milwaukee, WI) with a dedicated eight-channel breast coil. All patients underwent MR imaging in the prone position. MR imaging protocol included bilateral sagittal T2WI and a dynamic contrast-enhanced T1-weighted three-dimensional fast spoiled gradient-echo sequence with fat suppression (repetition time msec/echo time msec, 6.5/2.5; matrix size, 256×160; flip angle, 10°; field of view, 20×20 cm; section thickness, 1.5 mm; no gap). For all contrast-enhanced examinations, a bolus of gadolinium-based contrast material (MultiHance, BraccoImaging, Milan, Italy) was injected intravenously (0.1 mmol/L per kilogram of body weight), followed by a 20 mL saline solution flush. Thereafter, maximum-intensity projection, subtraction, and axial reformatted images were obtained. All lesions were clearly depicted at MR imaging.

MR image interpretation

All MR images of the 294 patients (DM group [$n = 147$] and control group [$n = 147$]) were randomly mixed and three dedicated breast radiologists (S.E.S., S.U.S., W.K.M., with 6, 3, and 23 years of experience, respectively) without the knowledge of clinical history independently reviewed the MR images using the 2013 Breast Imaging Reporting and Data System (BI-RADS) MR imaging lexicon [16]. The three reviewers were asked to determine the amount of fibroglandular tissue (FGT) and background parenchymal enhancement (BPE) which were assessed in the contralateral breast on the initial contrast-enhanced images or maximum-intensity projection images. The extent of disease was also evaluated as unifocal or multifocal and the lesion type as mass or non-mass enhancement (NME). For mass observations, shape, margin, internal enhancement patterns, and associated NME were assessed. The intratumoral signal intensity (SI) and peritumoral edema were also evaluated on T2WI as absent or present. High intratumoral SI on T2WI was visually determined when SI of the tumor was stronger than that of water or vessels or higher than that of the surrounding normal parenchymal glandular tissue [19]. Peritumoral edema was also visually defined when high SI around the tumor or posterior to the tumor mass in the prepectoral area was observed on T2WI [14, 20].

In addition, one radiologist (S.E.S.) with 6 years of experiences in breast imaging measured the distance from the nipple to the lesion, the distance from the skin to the lesion, and the distance from the chest wall to the lesion on the initial contrast-enhanced images [15]. For kinetic curve assessment, the time–signal intensity curve obtained from the pre-contrast and each post-contrast series using operator-defined regions of interest (ROI) within the tumor was used. The maximally enhancing ROI was selected for analysis. The kinetic curve patterns were categorized into three types (persistent, plateau, or washout).

Postoperative care and follow-up

After surgery, chemotherapy, hormonal therapy, and/or trastuzumab were administered according to the characteristics of a tumor of each patient. For the surveillance of DM, chest radiography, chest computed tomography (CT), and bone scan were annually performed in all patients as per our institutional practice. Whole-body fluorine 18 fluorodeoxyglucose positron emission tomography/CT were electively performed for patients with clinical symptoms of DM or suspicious DM on chest CT or bone scan. The DM sites were categorized as follows: bone; liver; lung; brain; or distant nodal (nodes beyond the ipsilateral axillary/internal mammary area/supraclavicular). In the case of

multiple DM, the DM site that was confirmed by biopsy or excision or initially detected on imaging studies was recorded. DM-free survival was defined as the interval between the date of breast cancer operation and the date of DM.

Statistical analysis

Patient and MR imaging characteristics between the DM group and control group and across the three breast cancer subtypes were compared using the Chi square test or Fisher's exact test for categorical variables and Wilcoxon rank sum test for continuous variables.

For statistical analysis, the categorical variables for breast MR imaging features were dichotomized into two categories each as follows: the amount of FGT (entirely fatty or scattered vs heterogeneous or extreme), BPE patterns (minimal or mild vs moderate or marked), mass shape (irregular vs round to oval), mass margin (not circumscribed vs circumscribed), mass internal enhancement (rim vs homogeneous or heterogeneous), intratumoral high SI on T2WI (present vs absent), and peritumoral edema (present vs absent). Breast MR imaging morphologic features were determined from the features at least two of the three interpreting breast radiologists classified. Interobserver variability was calculated to evaluate the categorical ratings by three reviewers with k statics. The strength of k agreement was defined as follows: poor ($k < 0$), slight ($k = 0.0$–0.20), fair ($k = 0.21$–0.40), moderate ($k = 0.41$–0.60), substantial ($k = 0.61$–0.80), and almost perfect ($k = 0.81$–1.00) [21]. Clinical–pathologic features were also dichotomized for statistical analysis as follows: age (≥ 50 years vs < 50 years), pathologic tumor type (lobular or other vs ductal), tumor stage (T3 vs T1-2), nodal stage (N2-3 vs N0-1), lymphovascular invasion (present vs absent), and Ki-67 index (≥ 14 vs $< 14\%$). We did not include histologic grade and pathologic stage in multivariate analysis since controlling for both histologic grade and Ki-67 index and both pathologic stage and T or N (which are tightly linked) could result in overfitting of the model.

We examined the associations of preoperative MR imaging and clinical–pathologic features with DM-free survival using Cox proportional hazard models. Hazard ratios (HR) and 95% confidence intervals (CI) for DM-free survival were calculated using univariate analysis, and variables with p values less than 0.30 in the univariate analysis and the use of systemic adjuvant therapy were selected as input variables for a multivariate model. All interactions between any two features in the final model were tested. Subgroup analysis was performed according to breast cancer stage and IHC subtype. The MR imaging feature found to differ significantly across the DM group

and control group was further estimated with the adjusted Kaplan–Meier method, and the survival times were compared using the log-rank test. We examined the association of the significant MR imaging feature with clinical–pathologic features using logistic regression analysis. Odds ratios (OR) and 95% CI were calculated using univariate logistic regression analysis, and variables with p values less than 0.30 were selected for the multivariate model.

All statistical analyses were performed using Statistical Package for the Social Sciences (SPSS, version 20; IBM, Armonk, NY) software; p values less than 0.05 were considered significant.

Results

Patient characteristics

Matched clinical–pathologic characteristics of the 294 patients are listed in Table 1. No significant differences were found between the DM group and control group with regard to the matched variables. The median age of the DM group and the control group was 47 years ($p = 1.000$). Both of the DM group and the control group comprised 13 patients with pathologic stage I (8.8%), 83 patients with stage II (56.5%), and 51 patients with stage III (34.7%). According to IHC results, 65 cases were HR-positive/HER2-negative, 39 cases were HER2-positive, and 43 cases were triple-negative in both the DM and control groups. With respect to the type of treatment, no significant differences were observed between the DM group and the control group with regard to surgery type and adjuvant treatment. The median follow-up time was 5.6 years (range, 0.9–11.5 years) for DM-free survival and the median time to DM was 2.9 years (range, 0.5–11.4 years). Of the 147 patients with DM, bone ($n = 48$) was the most frequent metastatic site followed by the lung ($n = 40$), liver ($n = 31$), distant nodal ($n = 16$), and brain ($n = 12$).

MR imaging features and interobserver agreement

For MR imaging features, rim enhancement and peritumoral edema were more frequently observed in the DM group compared with the control group (44.2 vs 25.2%, $p = 0.001$; 29.9 vs 20.4%, $p = 0.60$, respectively) (Figs. 1, 2). In the subgroup analysis, rim enhancement and peritumoral edema were most frequently observed in triple-negative tumors followed by HER2-positive and HR-positive/HER2-negative tumors. In HR-positive/HER2-negative tumors, the median distance from lesion to chest wall was 1.2 cm (range, 0–5.5 cm); that in DM group was

1.0 cm (range, 0—3.6 cm) and that in control group was 1.6 cm (range, 0–5.5 cm) ($p = 0.005$). Preoperative MR imaging features between DM and control groups according to IHC subtypes are summarized in Supplementary Table S1.

With regard to the evaluation of interobserver agreement between three reviewers, there was substantial overall agreement for FGT ($k = 0.62$ [95% CI 0.49–0.76]) and mass internal enhancement ($k = 0.62$ [95% CI 0.49–0.74]) and moderate agreement for BPE ($k = 0.59$ [95% CI 0.4–0.78]), multifocality ($k = 0.58$ [95% CI 0.44–0.73]), mass shape ($k = 0.53$ [95% CI 0.4–0.67]), mass margin ($k = 0.57$ [95% CI 0.4–0.74]), associated NME ($k = 0.47$ [95% CI 0.32–0.62]), intratumoral high SI ($k = 0.52$ [95% CI 0.34–0.71]), and peritumoral edema ($k = 0.46$ [95% CI 0.3–0.62]). Interobserver agreement for all MR imaging features was moderate to substantial.

MR imaging features associated with DM-free survival

In the multivariate analysis, rim enhancement (HR, 1.83 [95% CI 1.29, 2.51]; $p = 0.001$) and peritumoral edema (HR, 1.48 [95% CI 1.03, 2.11]; $p = 0.032$) were significant imaging features associated with worse DM-free survival in patients with invasive breast cancer. In the subgroup analysis according to breast cancer stage, MR imaging feature associated with DM-free survival in stage I or II breast cancers was rim enhancement (HR, 1.99, [95% CI 1.32, 3.00, $p = 0.001$) and that in stage III breast cancers was peritumoral edema (HR, 2.64, [95% CI 1.49, 4.68, $p = 0.001$). In the subgroup analysis according to breast cancer subtypes, DM-free survival was associated with rim enhancement (HR, 1.87 [95% CI 1.09, 3.07]; $p = 0.021$), peritumoral edema (HR, 2.61 [95% CI 1.30, 5.26]; $p = 0.007$), and the distance from the chest wall (HR, 0.73 [95% CI 0.56, 0.94]; $p = 0.015$) for HR-positive/HER2-negative tumors and rim enhancement (HR, 2.10 [95% CI 1.11, 3.95]; $p = 0.021$) for HER2-positive tumors. However, there was no MR imaging feature associated with DM-free survival in triple-negative tumors (Table 2).

Kaplan–Meier analysis revealed that rim enhancement and peritumoral edema were significantly associated with worse DM-free survival ($p < 0.001$ and $p < 0.001$, respectively) (Fig. 3). In subgroup analysis, rim enhancement, the presence of peritumoral edema, and the distance from the chest wall were significantly associated with worse DM-free survival ($p = 0.012$, $p = 0.030$ and $p = 0.001$, respectively) in HR-positive/HER2-negative tumors. Rim enhancement was significantly associated with worse DM-free survival in HER2-positive tumors ($p = 0.018$), but not in triple-negative tumors ($p = 0.119$).

Table 1 Matched patient characteristics

| Variables	All (n = 294)			HR-positive/HER2-negative tumors (n = 130)			HER2-positive tumors (n = 78)			Triple-negative tumors (n = 86)		
	DM group (n = 147)	Control group (n = 147)	p	DM group (n = 65)	Control group (n = 65)	p	DM group (n = 39)	Control group (n = 39)	p	DM group (n = 43)	Control group (n = 43)	p
Age			1.000			1.000			1.000			1.000
<50 years	90 (61.2)	90 (61.2)		43 (66.2)	43 (66.2)		24 (61.5)	24 (61.5)		23 (53.5)	23 (53.5)	
≥50 years	57 (38.8)	57 (38.8)		22 (33.8)	22 (33.8)		15 (38.5)	15 (38.5)		20 (46.5)	20 (46.5)	
Median age, years old (range)	47 (22–82)	47 (26–74)	1.000	46 (22–82)	46 (32–74)	0.860	48 (30–70)	49 (26–61)	0.650	45 (32–76)	46 (27–69)	1.000
Tumor type			1.000			1.000			1.000			1.000
Ductal	139 (94.6)	139 (94.6)		59 (90.8)	59 (90.8)		39 (100)	39 (100)		41 (95.3)	41 (95.3)	
Lobular/Other	8 (5.4)	8 (5.4)		6 (9.2)	6 (9.2)		0 (0)	0 (0)		2 (4.7)	2 (4.7)	
Histologic grade			1.000			1.000			1.000			1.000
I or II	42 (28.5)	42 (28.5)		32 (49.2)	32 (49.2)		5 (12.8)	5 (12.8)		5 (11.6)	5 (11.6)	
III	105 (71.5)	105 (71.5)		33 (50.8)	33 (50.8)		34 (87.2)	34 (87.2)		38 (88.4)	38 (88.4)	
Tumor stage			1.000			1.000			1.000			1.000
T1	27 (18.4)	27 (18.4)		9 (13.8)	9 (13.8)		10 (25.6)	10 (25.6)		8 (18.6)	8 (18.6)	
T2	103 (70.1)	103 (70.1)		47 (72.3)	47 (72.3)		27 (69.2)	27 (69.2)		29 (67.4)	29 (67.4)	
T3	17 (11.5)	17 (11.5)		9 (13.8)	9 (13.8)		2 (5.1)	2 (5.1)		6 (14.0)	6 (14.0)	
Median pathologic lesion size (range)	2.5 (1.0–7.5)	2.6 (1.2–9.0)	0.370	2.8 (0.8–7.5)	2.5 (1.2–8.5)	0.702	2.5 (0.9–5.5)	2.7 (0.2–7.5)	0.821	2.5 (1.5–6.5)	2.5 (0.6–9.0)	1.000
Nodal stage			1.000			1.000			1.000			1.000
0	56 (38.1)	56 (38.1)		22 (33.8)	22 (33.8)		12 (30.8)	12 (30.8)		24 (55.8)	24 (55.8)	
N1	43 (30.6)	43 (30.6)		23 (35.4)	23 (35.4)		10 (25.6)	10 (25.6)		10 (23.3)	10 (23.3)	
N2-3	46 (31.3)	46 (31.3)		20 (30.8)	20 (30.8)		17 (43.6)	17 (43.6)		9 (20.9)	9 (20.9)	
Stage			1.000			1.000			1.000			1.000
I	13 (8.8)	13 (8.8)		2 (3.1)	2 (3.1)		5 (12.8)	5 (12.8)		6 (14.0)	6 (14.0)	
II	83 (56.5)	83 (56.5)		39 (60.0)	39 (60.0)		17 (43.6)	17 (43.6)		27 (62.8)	27 (62.8)	
III	51 (34.7)	51 (34.7)		24 (36.9)	24 (36.9)		17 (43.6)	17 (43.6)		10 (23.3)	10 (23.3)	
Pathologic multifocality			0.196			0.410			1.000			0.195
Absent	127 (86.4)	134 (91.2)		56 (86.2)	59 (90.8)		36 (92.3)	35 (89.7)		35 (81.4)	40 (93.0)	
Present	20 (13.6)	13 (8.8)		9 (13.8)	6 (9.2)		3 (7.7)	4 (10.3)		8 (18.6)	3 (7.0)	
Lymphovascular invasion			1.000			1.000			1.000			1.000
Absent	50 (34.0)	50 (34.0)		25 (38.5)	25 (38.5)		9 (23.1)	9 (23.1)		16 (37.2)	16 (37.2)	
Present	97 (66.0)	97 (66.0)		40 (61.5)	40 (61.5)		30 (76.9)	30 (76.9)		27 (62.8)	27 (62.8)	

Table 1 continued

Variables	All (n = 294)			HR-positive/HER2-negative tumors (n = 130)			HER2-positive tumors (n = 78)			Triple-negative tumors (n = 86)		
	DM group (n = 147)	Control group (n = 147)	p	DM group (n = 65)	Control group (n = 65)	p	DM group (n = 39)	Control group (n = 39)	p	DM group (n = 43)	Control group (n = 43)	p
Ki-67 status			1.000			1.000			1.000			1.000
<14%	109 (74.1)	109 (74.1)		57 (87.7)	57 (87.7)		25 (64.1)	25 (64.1)		27 (62.8)	27 (62.8)	
≥14%	38 (25.9)	38 (25.9)		8 (12.3)	8 (12.3)		14 (35.9)	14 (35.9)		16 (37.2)	16 (37.2)	
Margin status			0.557			0.604			0.200			0.202
Clear	131 (89.1)	134 (91.2)		55 (84.6)	58 (89.2)		38 (97.4)	34 (87.2)		38 (88.4)	42 (97.7)	
Close	16 (10.9)	13 (8.8)		10 (15.4)	7 (10.8)		1 (2.6)	5 (12.8)		5 (11.6)	1 (2.3)	
IHC receptor status												
ER or PR-positive	76 (48.3)	76 (48.3)	1.000	65 (100)	65 (100)	1.000	11 (28.2)	11 (28.2)	1.000	0 (0)	0 (0)	1.000
HER2-positive	39 (26.5)	39 (26.5)	1.000	0 (0)	0 (0)	1.000	39 (100)	39 (100)	1.000	0 (0)	0 (0)	1.000
Operation method			0.080			0.160			1.000			0.116
Breast conserving surgery	68 (46.3)	83 (56.5)		30 (46.2)	38 (58.5)		14 (35.9)	14 (35.9)		24 (55.8)	31 (72.1)	
Mastectomy	79 (53.7)	64 (43.5)	0.117	35 (53.8)	27 (41.5)	0.403	25 (64.1)	25 (64.1)	0.615	19 (44.2)	12 (27.9)	0.397
Chemotherapy	142 (96.6)	136 (92.5)		63 (96.9)	61 (93.8)		38 (97.4)	36 (92.3)		41 (95.3)	39 (90.7)	
Aromatase inhibitor	32 (21.8)	40 (27.2)	0.278	30 (46.2)	33 (50.8)	0.599	2 (5.1)	7 (17.9)	0.154	0 (0)	0 (0)	1.000
Trastuzumab	23 (15.6)	19 (12.9)	1.000	0 (0)	0 (0)	1.000	23 (58.9)	19 (48.7)	1.000	0 (0)	0 (0)	1.000

HR hormone receptor, *ER* estrogen receptor, *PR* progesterone receptor, *HER2* human epidermal growth factor receptor 2

Fig. 1 Preoperative breast MR images of a 63-year-old woman who underwent breast conserving surgery for stage II (T2, 2.5 cm and N1, 3/23), high histologic grade, and HR-positive/HER2-negative breast cancer. **a** Sagittal contrast-enhanced T1-weighted image shows a round mass with rim enhancement in the *left* breast. **b** Sagittal T2-weighted image shows peritumoral edema (*arrowhead*) posterior to the mass. After a follow-up of 2.4 years, a soft tissue mass at the anterior mediastinum was found and confirmed as metastatic carcinoma by excision
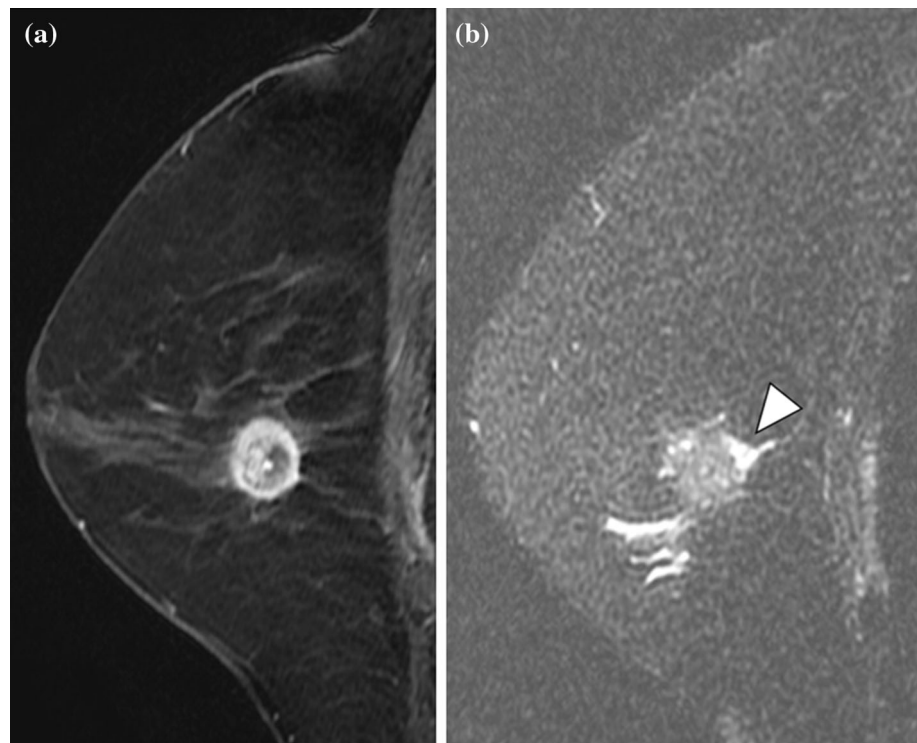
Fig. 2 Preoperative breast MR images of a 48-year-old woman who underwent mastectomy for stage II (T2, 3.5 cm and N1, 1/26), intermediate histologic grade, HR-positive/HER2-negative breast cancer. **a** Sagittal contrast-enhanced T1-weighted image shows an irregular, heterogeneously enhancing mass in the *left* breast. **b** Sagittal T2-weighted image shows no peritumoral edema. The patient was found to have no breast cancer metastasis after a follow-up of 7 years
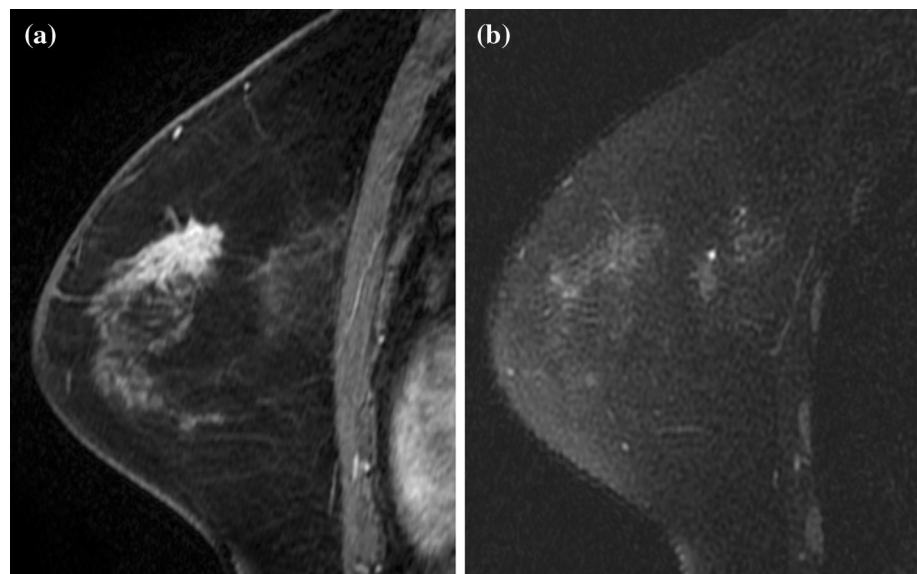
Clinical–pathologic variables associated with significant MR imaging features

Among the 7 clinical–pathologic variables, rim enhancement was significantly associated with high Ki-67 index (OR 2.71 [95% CI 1.53, 4.77]; $p = 0.001$), and low tumor stage (OR 0.22 [95% CI 0.08, 0.66]; $p = 0.007$) (Table 3). Peritumoral edema was significantly associated with high Ki-67 index (OR 2.59 [95% CI 1.45, 4.62]; $p = 0.001$), high nodal stage (OR 1.88 [95% CI 1.06, 3.32];

$p = 0.030$), and age ≥ 50 years (OR 1.82 [95% CI 1.05, 3.15]; $p = 0.033$).

Discussion

In this study, we compared the preoperative breast MR imaging features of breast cancer cohorts with and without DM after controlling for the clinical–pathologic variables known as risk factors for DM. Our study results showed

Table 2 Comparison of preoperative mr imaging features associated with distant metastasis (DM)-free survival according to breast cancer subtypes

Variables	All (n = 294)		HR-positive/HER2-negative tumors (n = 130)		HER2-positive tumors (n = 78)		Triple-negative tumors (n = 86)	
	Adjusted HR [95% CI]	p	Adjusted HR [95% CI]	p	Adjusted HR [95% CI]	p	Adjusted HR [95% CI]	p
MR imaging features								
Amount of fibroglandular tissue								
Background parenchymal enhancement					0.64 [0.25–1.64]	0.355		
Multifocality	1.33 [0.94-1.88]	0.097						
Mass shape								
Mass margin								
Mass internal enhancement	1.83 [1.29–2.51]	0.001	1.87 [1.09–3.07]	0.021	2.10 [1.11–3.95]	0.021	1.49 [0.80–2.79]	0.123
Associated NME								
Intratumoral high SI								
Peritumoral edema	1.48 [1.03–2.11]	0.032	2.61 [1.30–5.26]	0.007			1.37 [0.73–2.58]	0.321
Distance from nipple								
Distance from skin								
Distance from chest wall			0.73 [0.56–0.94]	0.015				
Tumor kinetics								
Adjuvant therapy								
Aromatase inhibitor	0.73 [0.49–1.10]	0.132	1.02 [0.61–1.73]	0.919	0.38 [0.09–1.60]	0.188		
Trastuzumab	1.19 [0.75–1.89]	0.450			1.01 [0.50–2.04]	0.961		

HR hazard ratio at multivariate analysis, *CI* confidence interval, *NME* non-mass enhancement, *SI* signal intensity
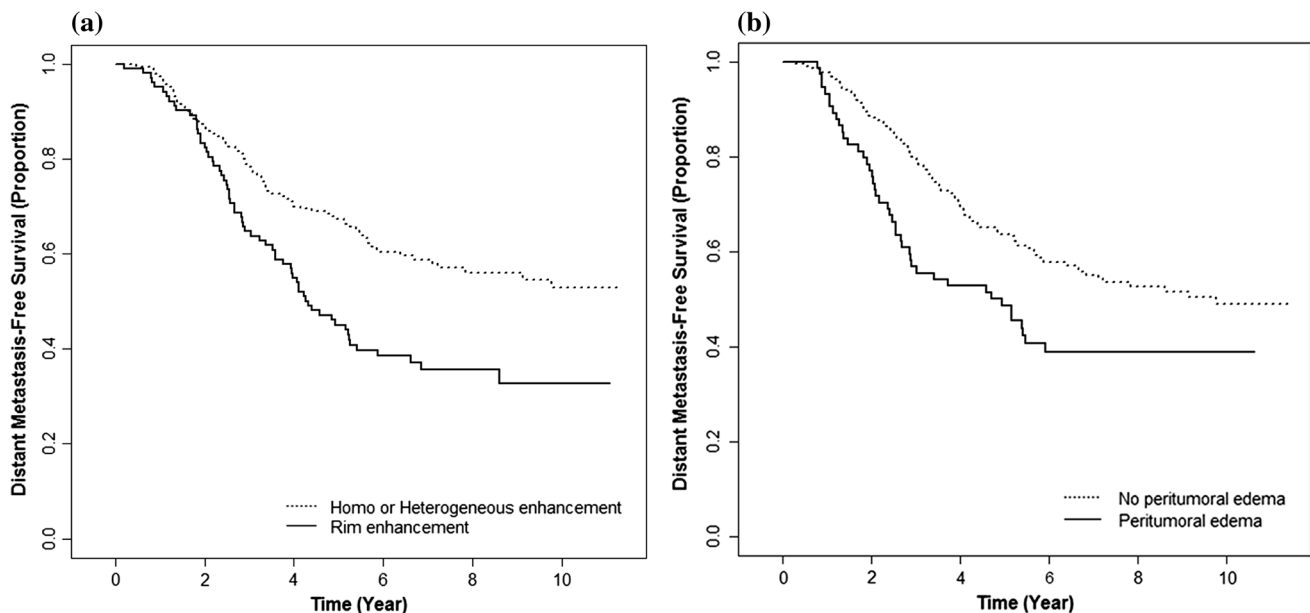
Fig. 3 Kaplan–Meier curves showing distant metastasis (DM)-free survival rate in 294 patients with breast cancer. **a** The *solid line* represents DM-free survival in patients with rim enhancement on preoperative MR images (n = 102); the *dashed line*, patients with homogeneous or heterogeneous enhancement (n = 192) (p < 0.001). **b** The *solid line* represents DM-free survival in patients with peritumoral edema (n = 74); the dashed line, patients without peritumoral edema (n = 220) (p < 0.001)

Table 3 Clinical–pathologic characteristics of rim enhancement and associated features in 294 patients

Variables	Rim enhancement				Peritumoral edema			
	Univariate analysis		Multivariate analysis		Univariate analysis		Multivariate analysis	
	Unadjusted OR [95% CI]	p	Adjusted OR [95% CI]	p	Unadjusted OR [95% CI]	p	Adjusted OR [95% CI]	p
Age								
≥50 years versus <50 years	1.49 [0.91–2.44]	0.105			1.85 [1.09–3.16]	0.022	1.82 [1.05–3.15]	0.033
Pathologic tumor type								
Lobular/other versus ductal	0.22 [0.07–0.64]	0.251			0.35 [0.07–1.57]	0.260		
Pathologic tumor stage								
T3 versus T1-2	0.22 [0.07–0.64]	0.003	0.22 [0.08–0.66]	0.007	1.27 [0.57–2.81]	0.545		
Pathologic nodal stage								
N2-3 versus N0-1	0.37 [0.20–0.66]	0.001			1.73 [1.00–3.00]	0.047	1.88 [1.06–3.32]	0.030
Pathologic multifocality								
Present versus absent	1.08 [0.51–2.30]	0.831			0.63 [0.25–1.59]	0.326		
Lymphovascular invasion								
Present versus absent	0.75 [0.45–1.24]	0.265			1.54 [0.86–2.76]	0.143		
Ki-67 status								
≥14% versus <14%	2.40 [1.40–4.11]	0.001	2.71 [1.53–4.77]	0.001	2.57 [1.46–4.54]	0.001	2.59 [1.45–4.62]	0.001

OR odds ratio, *CI* confidence interval

that preoperative MR imaging features of rim enhancement and peritumoral edema were more common in the DM group compared with the control group and were associated with worse DM-free survival in patients with breast cancers. Interestingly, significant imaging features associated with worse DM-free survival were different between breast cancer subtypes and stages. DM-free survival was associated with rim enhancement, peritumoral edema, and the distance from the chest wall for HR-positive/HER2-negative tumors and rim enhancement for HER2-positive tumors. However, there was no MR imaging feature associated with DM-free survival in triple-negative tumors. These results may be explained by the more frequent incidence of these MR imaging features in aggressive triple-negative tumors than in HR-positive/HER2-negative or HER2-positive tumors, regardless of the presence of DM. For example, in our study, 51.1% (22/43) of those in the DM group and 37.2% (16/43) of those in the control group had rim enhancement in triple-negative tumors, while 36.9% (24/65) of those in the DM group and 20.0% (13/65) of those in the control group in HR-positive/HER2-negative tumors and 48.7% (19/39) of those in the DM group and 20.5% (8/39) of those in the control group in HER2-positive tumors had rim enhancement. In contrast to previous studies, BPE was not associated with DM-free survival in this study [16, 17]. To our knowledge, this is the first study to report MR imaging features associated with

DM-free survival according to IHC subtypes in patients with breast cancer.

We further examined the association of the significant MR imaging features with clinical–pathologic variables using logistic regression analysis. Our study results showed that rim enhancement and peritumoral edema were most significantly associated with high Ki-67 index of breast cancer. This finding is concordant with previous studies investigating relationships between breast MR imaging findings and prognostic markers of breast cancer [22–25]. Of note is that rim enhancement was associated with low pathologic stage, which suggests the usefulness of this finding particularly in early-stage breast tumors. The association of rim enhancement on DM-free survival is also supported by recent radiogenomic research by Yamamoto et al. [26] in which the enhancing rim fraction score of tumor, a quantitative MR imaging feature, was associated with HOX transcript antisense intergenic RNA (HOTAIR), known as a predictor of metastatic progression. Peritumoral edema, likely caused by increased vascular permeability and the release of tumor-associated cytokines and growth factors, has been associated with poor recurrence-free survival after neoadjuvant therapy in patients with breast cancer [14, 25, 27]. In our study, peritumoral edema was the MR imaging feature associated with DM-free survival in stage III breast cancers. In The Cancer Genome Atlas and The Cancer Imaging Archive study

[28, 29], rim enhancement was associated with ER status and the activity of multiple genes related to the phospho-inositide 3 kinase (PI3K) pathway, which leads to cell growth and tumor proliferation and plays a significant role in endocrine resistance in breast cancer. Peritumoral edema was associated with Aurora A/GADD45A, BCL2L1, CCNE1, and FOXA1, which are related to resistance to chemotherapy and distant metastasis. In addition, TP53 mutation status, the most prevalent cancer driver event in breast cancer has been associated with rim enhancement and peritumoral edema [29, 30].

Previous studies with MR imaging reported that BRCA1-associated or familial breast cancers more frequently had a posterior or prepectoral location reflecting a greater tendency to spread to distant organs without axillary nodal involvement in aggressive triple-negative tumors compared with HR-positive/HER2-negative tumors [15, 31]. Anatomical and lymphoscintigraphic studies have revealed that tumors in the posterior locations have considerable lymphatic dissemination to the internal mammary node chain, which is the most important destination for lymph drainage outside of the axilla [32]. In our study, however, similar to rim enhancement and peritumoral edema, the distance from the chest wall was associated with DM-free survival in HR-positive/HER2-negative tumors but not in triple-negative tumors. A posterior or prepectoral location of breast cancer was associated with younger age, low nodal stage, and high histologic grade. This finding is concordant with the MR imaging study of tumor location using 1201 breast cancers in which age, mammographic density, axillary nodal status, and triple-negative status are significantly associated with absolute and normalized distances from the chest wall [15].

Our study had several limitations. First, our study cohort was retrospectively collected from a single tertiary academic institution and selection bias is inevitable. We did not match for the surgery type or the type of adjuvant therapy, and these factors could have affected survival outcome. However, our treatment strategy based on clinical–pathologic characteristics has not substantially changed during the study period. Second, we used qualitative assessments of MR imaging features, all of which had potentially inter- and intra-observer variability. We provided k-values interobserver variation in the assessment of rim enhancement and of peritumoral edema. Interobserver agreement was substantial ($k = 0.62$) for mass internal enhancement but only moderate ($k = 0.46$) for peritumoral edema. Because patients in our cohort underwent breast MR imaging after core needle biopsy, some findings of peritumoral edema may have been confused with changes after biopsy. Lastly, our study might have been underpowered to generalize the associations between MR imaging features in breast cancer subtypes and DM risk. In particular, the lack of a significant association of rim enhancement and DM-free survival outcome in triple-negative tumors might be due to the marked heterogeneity and the relatively small numbers of cases in this study [33, 34]. Further validation in multi-institutional, prospective studies is needed to confirm the utility of MR imaging biomarkers in clinical practice.

In conclusion, our study suggests that preoperative MR imaging features of rim enhancement and peritumoral edema were associated with worse DM-free survival in patients with breast cancer. The significant MR imaging features, however, were different between breast cancer subtypes and stages reflecting inter-tumor heterogeneity. Preoperative breast MR imaging features may be used as prognostic biomarkers that help predict DM risk in patients with breast cancer, especially in HR-positive/HER2-negative or HER2-positive tumors, thereby potentially enabling improved personalized treatment strategies for individual patients.

Compliance with Ethical Standards

Conflict of interest The authors declare no potential conflicts of interest.

Ethical approval All procedures performed in studies involving human participants were in accordance with the ethical standards of the institutional and/or national research committee and with the 1964 Helsinki declaration and its later amendments or comparable ethical standards.

Informed consent For this type of study formal consent is not required.

References

1. Early Breast Cancer Trialists' Collaborative Group (EBCTCG) (2005) Effects of chemotherapy and hormonal therapy for early breast cancer on recurrence and 15-year survival: an overview of the randomised trials. Lancet 365(9472):1687–1717

2. Weigelt B, Peterse JL, van't Veer LJ (2005) Breast cancer metastasis: markers and models. Nat Rev Cancer 5(8):591–602

3. Page DL (1991) Prognosis and breast cancer. recognition of lethal and favourable prognostic types. Am J Surg Pathol 15(4):334–349

4. Elston CW, Ellis IO (1991) Pathological prognostic factors in breast cancer. I. the value of histological grade in breast cancer: experience from a large study with long-term follow-up. Histopathology 19(5):403–410

5. Slamon DJ, Leyland-Jones B, Shak S, Fuchs H, Paton V, Bajamonde A, Fleming T, Eiermann W, Wolter J, Pegram M, Baselga J, Norton L (2001) Use of chemotherapy plus a monoclonal antibody against HER2 for metastatic breast cancer that overexpresses HER2. N Engl J Med 344(11):783–792

6. Klintman M, Bendahl PO, Grabau D, Lövgren K, Malmström P, Fernö M, South Sweden Breast Cancer Group (2010) The prognostic value of Ki67 is dependent on estrogen receptor status and histological grade in premenopausal patients with node-negative breast cancer. Mod Pathol 23(2):251–259

7. Wang Y, Klijn JG, Zhang Y, Sieuwerts AM, Look MP, Yang F, Talantov D, Timmermans M, Meijer-van Gelder ME, Yu J, Jatkoe T, Berns EM, Atkins D, Foekens JA (2005) Gene-expression profiles to predict distant metastasis of lymph-node-negative primary breast cancer. Lancet 365(9460):671–679

8. Goldhirsch A, Winer EP, Coates AS, Gelber RD, Piccart-Gebhart M, Thürlimann B, Senn HJ, Panel members (2013) Personalizing the treatment of women with early breast cancer: highlights of the St Gallen International Expert Consensus on the Primary Therapy of Early Breast Cancer 2013. Ann Oncol 24(9):2206–2223

9. Mauriac L, Keshaviah A, Debled M, Mouridsen H, Forbes JF, Thürlimann B, Paridaens R, Monnier A, Láng I, Wardley A, Nogaret JM, Gelber RD, Castiglione-Gertsch M, Price KN, Coates AS, Smith I, Viale G, Rabaglio M, Zabaznyi N, Goldhirsch A, BIG 1–98 Collaborative Group, International Breast Cancer Study Group (2007) Predictors of early relapse in postmenopausal women with hormone receptor-positive breast cancer in the BIG 1-98 trial. Ann Oncol 18(5):859–867

10. Goss PE, Ingle JN, Pritchard KI, Robert NJ, Muss H1, Gralow J, Gelmon K, Whelan T, Strasser-Weippl K, Rubin S, Sturtz K, Wolff AC, Winer E, Hudis C, Stopeck A, Beck JT, Kaur JS, Whelan K, Tu D, Parulekar WR (2016) Extending aromatase-inhibitor adjuvant therapy to 10 years. N Engl J Med 20; 375(16):1590–1591

11. Grimm LJ (2016) Breast MRI radiogenomics: current status and research implications. J Magn Reson Imaging 43(6):1269–1278

12. Li SP, Makris A, Beresford MJ, Taylor NJ, Ah-See ML, Stirling JJ, d'Arcy JA, Collins DJ, Kozarski R, Padhani AR (2011) Use of dynamic contrast-enhanced MR imaging to predict survival in patients with primary breast cancer undergoing neoadjuvant chemotherapy. Radiology 260(1):68–78

13. Schmitz AM, Loo CE, Wesseling J, Pijnappel RM, Gilhuijs KG (2014) Association between rim enhancement of breast cancer on dynamic contrast-enhanced MRI and patient outcome: impact of subtype. Breast Cancer Res Treat 148(3):541–551

14. Uematsu T, Kasami M, Watanabe J (2014) Is evaluation of the presence of prepectoral edema on T2-weighted with fat-suppression 3 T breast MRI a simple and readily available noninvasive technique for estimation of prognosis in patients with breast cancer? Breast Cancer 21(6):684–692

15. Kim WH, Han W, Chang JM, Cho N, Park IA, Moon WK (2015) Location of triple-negative breast cancers: comparison with estrogen receptor-positive breast cancers on MR imaging. PLoS ONE 10(1):e0116344. doi:10.1371/journal.pone.0116344.eCollection

16. Choi JS, Ko ES, Ko EY, Han BK, Nam SJ (2016) Background parenchymal enhancement on preoperative magnetic resonance imaging: association with recurrence-free survival in breast cancer patients treated with neoadjuvant chemotherapy. Medicine (Baltimore) 95(9):e3000. doi:10.1097/MD.0000000000003000

17. van der Velden BH, Dmitriev I, Loo CE, Pijnappel RM, Gilhuijs KG (2015) Association between parenchymal enhancement of the contralateral breast in dynamic contrast-enhanced MR imaging and outcome of patients with unilateral invasive breast cancer. Radiology 276(3):675–685

18. Yi A, Cho N, Yang KS, Han W, Noh DY, Moon WK (2015) Breast cancer recurrence in patients with newly diagnosed breast cancer without and with preoperative MR imaging: a matched cohort study. Radiology 276(3):695–705

19. Morris EA, Comstock CE, Lee CH et al (2013) ACR BI-RADS Magnetic resonance imaging. In: ACR BI-RADS® Atlas (ed) Breast imaging reporting and data system. American College of Radiology, Reston

20. Baltzer PA, Yang F, Dietzel M, Herzog A, Simon A, Vag T, Gajda M, Camara O, Kaiser WA (2010) Sensitivity and specificity of unilateral edema on T2w-TSE sequences in MR-mammography considering 974 histologically verified lesions. Breast J 16(3):233–239

21. Landis JR, Koch GG (1977) The measurement of observer agreement for categorical data. Biometrics 33(1):159–174

22. Szabo BK, Aspelin P, Kristoffersen WM, Tot T, Bone B (2003) Invasive breast cancer: correlation of dynamic MR features with prognostic factors. Eur Radiol 13(11):2425–2435

23. Lee SH, Cho N, Kim SJ, Cha JH, Cho KS, Ko ES, Moon WK (2008) Correlation between high resolution dynamic MR features and prognostic factors in breast cancer. Korean J Radiol 9(1):10–18

24. Matsubayashi R, Matsuo Y, Edakuni G, Satoh T, Tokunaga O, Kudo S (2000) Breast masses with peripheral rim enhancement on dynamic contrast-enhanced MR images: correlation of MR findings with histologic features and expression of growth factors. Radiology 217(3):841–848

25. Uematsu T (2015) Focal breast edema associated with malignancy on T2-weighted images of breast MRI: peritumoral edema, prepectoral edema, and subcutaneous edema. Breast Cancer 22(1):66–70

26. Yamamoto S, Han W, Kim Y, Du L, Jamshidi N, Huang D, Kim JH, Kuo MD (2015) Breast cancer: radiogenomic biomarker reveals associations among dynamic contrast-enhanced MR imaging, long noncoding RNA, and metastasis. Radiology 275(2):384–392

27. Bae MS, Shin SU, Ryu HS, Han W, Im SA, Park IA, Noh DY, Moon WK (2016) Pretreatment MR imaging features of triple-negative breast cancer: association with response to neoadjuvant chemotherapy and recurrence-free survival. Radiology 281(2): 392–400

28. Rao A, Net J, Brandt K, Huang E, Freymann J, Burnside E, Kirby J, Morris E, Bonaccio E, Giger M, Jaffe C, Ganott M, Sutton E, Le-Petross H, Zuley M, Dogan B, Whitman G (2015) TU-CD-BRB-07: identification of associations between radiologist-annotated imaging features and genomic alterations in breast invasive carcinoma, a TCGA phenotype research group study. Med Phys 42:3603–3604. doi:10.1118/1.4925592

29. Zhu Y, Li H, Guo W, Drukker K, Lan L, Giger ML, Ji Y (2015) Deciphering genomic underpinnings of quantitative MRI-based radiomic phenotypes of invasive breast carcinoma. Sci Rep 5:17787

30. Cancer Genome Atlas Network (2012) Comprehensive molecular portraits of human breast tumours. Nature 490(7418):61–70

31. Schrading S, Kuhl CK (2008) Mammographic, US, and MR imaging phenotypes of familial breast cancer. Radiology 246(1): 58–70

32. Tanis PJ, van Rijk MC, Nieweg OE (2005) The posterior lymphatic network of the breast rediscovered. J Surg Oncol 91(3): 195–198

33. Lehmann BD, Bauer JA, Chen X, Sanders ME, Chakravarthy AB, Shyr Y, Pietenpol JA (2011) Identification of human triple-negative breast cancer subtypes and preclinical models for selection of targeted therapies. J Clin Invest 121(7):2750–2767

34. Bae MS, Park SY, Song SE, Kim WH, Lee SH, Han W, Park IA, Noh DY, Moon WK (2015) Heterogeneity of triple-negative breast cancer: mammographic, US, and MR imaging features according to androgen receptor expression. Eur Radiol 25(2): 419–427